Physicochem. Probl. Miner. Process., 62(5), 2026, 235697

http://www.journalssystem.com/ppmp

Physicochemical Problems of Mineral Processing

ISSN 1643-1049
© Wroclaw University of Science and Technology

Role of flocculant dosage and water chemistry in governing sedimentation and filtration behaviour of sulphidic iron ore tailings

Argun Çiper [1,2], Yunus Emre Çavdar [1], Buse Sarmısak [1], Taha Boyraz [3], Feridun Boylu [1], Orhan Ozdemir [1]

[1] Department of Mineral Processing Engineering, Faculty of Mines, Istanbul Technical University, 34469, Istanbul, Türkiye

[2] YON Process Filtration Technology Machinery Engineering Industry and Trade Ltd. Co., 54400, Sakarya, Türkiye

[3] Department of Mining Engineering, Faculty of Engineering, Karadeniz Technical University, 61080, Trabzon, Türkiye

Corresponding author: orhanozdemir@itu.edu.tr (Orhan Ozdemir)

Abstract: Efficient solid-liquid separation of fine tailings is essential for improving water recovery and tailings management in mineral processing. In this study, the combined effects of flocculant dosage and water chemistry on sedimentation, floc size evolution, and pressure filtration behavior of sulfide iron ore tailings were investigated. A representative tailings sample from a concentrator, characterised by XRF, XRD, and SEM-EDS, was treated with a commercial anionic polyacrylamide-based flocculant using pure water and plant process water. Sedimentation performance was evaluated using interface height and supernatant turbidity; floc size evolution was monitored by laser diffraction; and pressure filtration tests were conducted at 7 bar using filter chambers with thicknesses of 25, 32, and 40 mm. The results showed that the addition of the flocculant significantly improved settling and clarification compared with the unconditioned suspension. A dosage of 30 g/Mg produced the most compact sediment bed and the most shear-resistant flocs, while increasing the dosage to 60 g/Mg further reduced supernatant turbidity, particularly in process water. At 120 g/Mg, excessive polymer addition partially restabilized the suspension and increased floc breakage, resulting in higher supernatant turbidity. Pure water consistently promoted faster settling, whereas process water provided better clarification at intermediate dosages, consistent with obtained zeta potential measurements indicating electrical double-layer compression and cation-mediated aggregation. Pressure filtration tests showed that increasing chamber thickness increased cumulative filtrate recovery, reaching 32.30% for the 40 mm chamber, while final cake moisture remained similar for all chamber configurations. Overall, 30 g/Mg was identified as the optimum flocculant dosage, providing the best balance between settling, sediment consolidation, floc stability, and filtration performance. These findings show that recycled process water can be used effectively without compromising dewatering performance.

Keywords: tailings, flocculation, anionic polyacrylamide, process water, pressure filtration, dewatering

1. Introduction

Mineral processing operations are predominantly conducted using wet methods, which use large amounts of water during grinding, classification, separation, and slurry transport. As a consequence, large volumes of aqueous waste streams containing fine particles and non-commercial materials are generated as mine tailings. Excessive water consumption in the mining industry has led to the continuous accumulation of high-moisture tailings. Currently, more than 10 billion tons of mine tailings are produced annually worldwide, and this amount is projected to increase significantly in the coming decades (Araya et al., 2021). Water is consumed in various operational activities, including ore processing, dust suppression, and tailings transportation, making water management a critical challenge for sustainable mining practices (Ossa-Moreno et al., 2018). Consequently, efficient dewatering and water recovery systems have become essential for improving environmental performance and operational sustainability.

DOI: 10.37190/ppmp/235697

Dewatering of mineral tailings is a fundamental stage in mining and mineral processing operations, particularly amid increasing global water scarcity (Dash et al., 2011; Lee et al., 2006). Various mechanical dewatering technologies, including dewatering screens, thickeners, centrifuges, vacuum filters, and pressure filtration systems, are widely applied to reduce the moisture content of concentrates and tailings (Dias et al., 2003; Häkkinen & Ekberg, 2009). In this context, researchers have widely investigated filtration for iron ore products and tailings because it can improve water recovery and reduce the moisture content of dewatered solids (Amarante et al., 2002; Dash et al., 2011; Dias et al., 2003). Among these technologies, pressure filtration systems are particularly relevant to the present study, as laboratory-scale filter press tests were used to evaluate cake formation, filtrate recovery, and final cake moisture under controlled conditions.

Filtration efficiency can be further enhanced through chemical conditioning using filtration aids such as flocculants, surfactants, and coagulants (Qi et al., 2011). These additives influence slurry characteristics by modifying zeta potential, surface chemistry, coagulation behaviour, floc formation, and rheological properties (Amarante et al., 2002; McGuire et al., 2006). Filtration performance is commonly evaluated using parameters such as filtrate rate, specific cake resistance, cake formation rate, moisture content, and filter cloth resistance (Qi et al., 2011).

Sedimentation of mining pulps is strongly governed by interparticle forces caused by surface charge characteristics. The balance between attractive and repulsive forces determines particle aggregation behaviour, which can be influenced by slurry pH, ionic environment, and surface chemistry (Johnson et al., 2000; McGuire et al., 2006). Under favourable chemical conditions, reduced electrostatic repulsion can promote particle aggregation, thereby improving filtration rates and reducing cake moisture (Dias et al., 2003; McGuire et al., 2006).

Fine-particle suspensions in mineral processing tailings generally remain stable and resist aggregation because of electrochemical interactions in aqueous environments (Li et al., 2013). To overcome this stability, coagulation and flocculation are commonly used to destabilize suspensions. In coagulation, electrolytes or oppositely charged species can reduce electrostatic repulsion by altering the ionic environment around particles, thereby promoting aggregation through short-range attractive forces (Johnson et al., 2000; Palomino et al., 2012). In contrast, flocculation uses long-chain polymeric flocculants that bind dispersed particles and promote rapid settling via polymer bridging (Gregory & Barany, 2011).

Long-chain organic polymer flocculants are used to aggregate and rapidly settle fine particles in mineral processing suspensions. These polymers may be anionic, cationic, or non-ionic. Flocculation occurs through several mechanisms, including polymer bridging, charge neutralization, electrostatic patch formation, and depletion flocculation (Zhu et al., 2009). The efficiency of these mechanisms depends strongly on flocculant properties such as molecular weight, charge density, and functionality, as well as slurry characteristics including particle size distribution, surface charge, solution chemistry, pH, ionic strength, and hydrodynamic conditions (Sworska et al., 2000a, 2000b).

Operational parameters such as solids concentration, mixing intensity, and conditioning time also affect flocculation performance. These parameters govern the formation of flocs with different physical characteristics, including size, structure, and mechanical strength, which directly affect subsequent solid-liquid separation processes (Alam et al., 2011; Gungoren et al., 2020; Jarvis et al., 2005; Parekh, 2009). Different dewatering operations require flocs with specific properties; strong, high-density flocs are generally preferred for filtration, whereas more open-structured flocs suit sedimentation (Alam et al., 2011; Jarvis et al., 2005).

During industrial dewatering operations, flocs are frequently exposed to hydrodynamic and mechanical stresses, which may lead to floc breakage and size reduction. Although limited breakage may facilitate reagent redistribution, excessive fragmentation generally harms dewatering performance, as smaller particles settle more slowly and filter less well. Consequently, floc strength represents an important parameter for efficient sedimentation. However, under industrial conditions, pumping, agitation, and slurry transfer may partially modify the floc structure formed during conditioning. Therefore, filtration performance should not be attributed solely to the initial floc size, but rather to the combined effects of floc strength, shear resistance, slurry rheology, and the resulting cake structure (Hogg, 2000; Jarvis et al., 2005; Sworska et al., 2000b).

Compared with coagulation, flocculation generally produces larger, more robust aggregates, particularly when high-molecular-weight polymers are used (Ozkan et al., 2016). Flocculants enhance particle bonding, reduce degradation rates, and promote floc growth (Hogg, 2000). Furthermore, synergistic interactions between flocculants and dissolved ions can further improve floc strength and stability, even under highly turbulent conditions, thereby enhancing overall dewatering efficiency (Negro et al., 2006; Wang et al., 2014).

In filtration processes, flocculant conditioning significantly influences performance. Although flocculation improves filtration kinetics and cake permeability, excessive reagent use can substantially increase operating costs (Alam et al., 2011). Therefore, determining the optimal flocculant dosage and charge type is economically important to obtain filter cakes with low moisture content and a sufficiently clear filtrate suitable for process water recycling.

Despite extensive research on flocculation and dewatering, most studies have focused on either sedimentation or filtration, each conducted under laboratory-scale conditions. Limited attention has been paid to evaluating settling behavior and pressure filtration performance together using industrial tailings under realistic operating conditions. In this context, a detailed understanding of the relationship between flocculation parameters, settling kinetics, and filtration efficiency remains necessary. Accordingly, this study investigates how flocculant dosage and water chemistry affect the sedimentation and pressure filtration performance of sulfide iron ore tailings. Sedimentation tests, floc size measurements, and laboratory-scale filter press experiments were conducted to evaluate the relationships among floc structure, settling behavior, and filtration efficiency.

2. Materials and methods

2.1. Materials

A representative sulphide iron ore tailings sample was obtained from an operating concentrator plant in Türkiye and used throughout the study. The sample's chemical composition was determined by X-ray fluorescence (XRF) (WD-XRF, Zetium, Malvern Panalytical, London, UK) analysis. Table 1 presents the sample's chemical composition. The results indicate that the sample is primarily composed of SiO_2 (46.2%), Fe_2O_3 (11.8%), and Al_2O_3 (10.6%). In addition, CaO, MgO, and K_2O contents are 8.6%, 4.4%, and 3.7%, respectively. Minor amounts of MnO (0.1%) and CuO (0.1%) were also detected.

Table 1. Chemical composition of the representative tailings sample determined by XRF analysis

SiO_2 (%)	Fe_2O_3 (%)	Al_2O_3 (%)	CaO (%)	MgO (%)	K_2O (%)	SO_3 (%)	Na_2O (%)	TiO_2 (%)	P_2O_5 (%)	MnO (%)	CuO (%)
46.2	11.8	10.6	8.6	4.4	3.7	2.0	1.7	0.4	0.1	0.1	0.1
Cl (ppm)	**BaO (ppm)**	**WO_3 (ppm)**	**Co_3O_4 (ppm)**	**SrO (ppm)**	**ZrO_2 (ppm)**	**Rb_2O (ppm)**	**Cr_2O_3 (ppm)**	**ZnO (ppm)**	**As_2O_3 (ppm)**	**PbO (ppm)**	**LOI* (%)**
915.7	843.5	339.5	300.1	283.6	200.2	192.8	159.4	124.5	117.2	74.2	10.0

*LOI: Loss on ignition

Mineralogical composition of the sample was characterized using X-ray diffraction (XRD) (Panalytical X'Pert³ Powder, Malvern Panalytical, London, UK). As shown in Fig. 1, the XRD pattern indicates that the sample consists mainly of silicate minerals, with quartz and K-feldspar as the dominant crystalline phases. Albite and orthoclase were also identified as feldspar-group minerals, giving characteristic reflections primarily between 22° and 35° 2θ. In addition, minor amounts of magnetite and chalcopyrite were detected, with their characteristic reflections observed at approximately 30° and 35° 2θ for magnetite and near 29° 2θ for chalcopyrite.

The particle size distribution was determined using a laser diffraction particle size analyzer (Malvern Mastersizer 2000, Malvern Panalytical, London, UK). Particle size analysis yielded d_{90}, d_{50}, and d_{10} values of ~63 μm, ~17 μm, and ~2.5 μm, respectively. Fig. 2 shows the particle size distribution of the sample.

The morphology and chemical composition of the sample were examined by scanning electron microscopy coupled with energy-dispersive X-ray spectroscopy (SEM-EDS) using an Apreo 2S (Thermo Fisher Scientific) at an acceleration voltage of 20 kV. Both area and point analyses were performed on

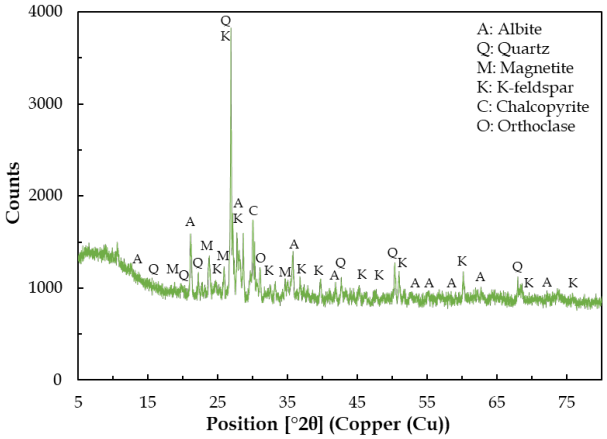

Fig. 1. XRD pattern of the sample

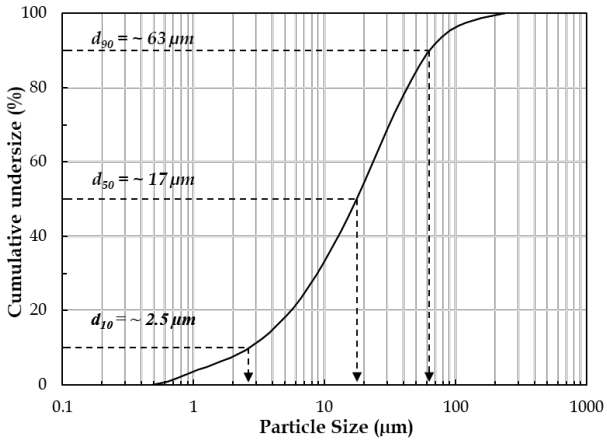

Fig. 2. Particle size distribution of representative ore sample

different regions of the sample. Representative SEM micrographs are shown in Fig. 3, while the elemental compositions of the selected areas and points are summarised in Table 2. The sample is composed predominantly of angular and irregularly shaped particles spanning a broad size range, consistent with the particle size distribution shown in Fig. 2. EDS area analyses revealed that the particle matrix is mainly composed of O, Si, Al, Mg, Ca, K, Na, and Fe, with oxygen and silicon contents ranging from 48.7 to 50.5% and 20.0 to 21.9%, respectively. These results indicate that the tailings are dominated by quartz, along with Mg-, Al-, and Ca-bearing silicate minerals. Point analyses further identified individual quartz grains containing up to 43.2% Si and 53.8% O, an iron oxide phase with 59.0% Fe (Fig. 3b), and residual sulphide minerals, including a pyrite grain containing 39.9% S and 49.9% Fe (Fig. 3c) and Cu-Fe sulphide (chalcopyrite-type) particles containing 19.9 to 20.7% Cu, 11.9 to 13.7% S, and 15.6 to 17.0% Fe (Fig. 3d). The occurrence of residual pyrite and chalcopyrite within a silicate-rich gangue is consistent with the sulphide iron ore origin of the tailings.

Table 2. Elemental compositions (%) of representative areas and points of the sample determined by SEM-EDS

Element	Silicate Matrix (area)	Quartz (point)	Iron Oxide (area)	Pyrite (point)	Cu-Fe Sulphide (point)
O	48.7	53.8	29.2	-	21.1
Si	20	43.2	4.7	4	6.2
Al	6.5	0.1	1.3	1.3	2.1
Fe	7.7	0.3	59	49.9	17
S	-	-	0.4	39.9	13.7
Cu	0.3	-	-	-	20.7
Mg	5.2	0.1	0.6	-	0.7
Ca	4.6	-	1.2	0.4	2.1

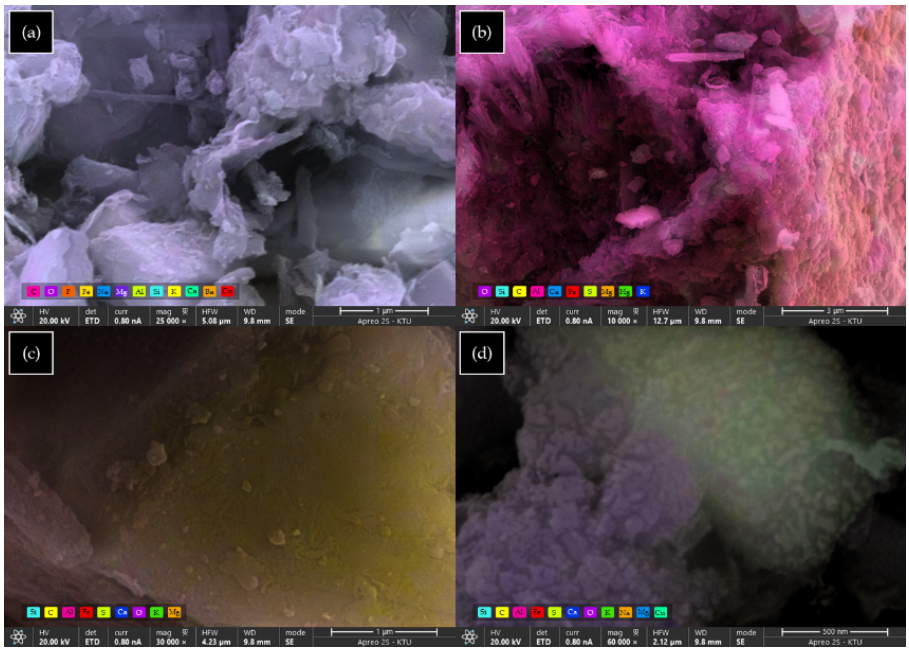

Fig. 3. SEM micrographs of the sample: (a) general view of the particles, (b) iron oxide particle, (c) pyrite grain, (d) Cu-Fe sulphide (chalcopyrite-type) bearing aggregate

Two different water types were used throughout the sedimentation experiments: pure water (TDS: 0 ppm) and process water. Pure water was used as a reference medium, while process water was used to evaluate the influence of water chemistry on flocculation and sedimentation behaviour. The ionic composition of the process water used in this study was determined by ICP-OES analysis. Table 3 presents the results. The process water used in the flocculation experiments contained relatively high concentrations of dissolved calcium, sodium, and potassium (236.9, 181.6, and 70.2 ppm, respectively). Magnesium was present at a much lower concentration (0.878 ppm), while trace metals, including zinc (0.01 ppm), iron (0.04 ppm), copper (0.009 ppm), and manganese (0.005 ppm), were very low. The process water was obtained from the clarified supernatant of the tailings slurry. Prior to the experiments, the slurry was allowed to settle naturally, resulting in solid-liquid separation. The supernatant phase was carefully decanted and used directly in the experiments without further treatment.

Table 3. Ionic composition of the process water

Ca (ppm)	Na (ppm)	K (ppm)	Mg (ppm)	Zn (ppm)	Fe (ppm)	Cu (ppm)	Mn (ppm)
236.9	181.6	70.2	0.878	0.01	0.04	0.009	0.005

A commercial anionic polyacrylamide (PAM)-based polymer (Dkloc 2034, Değişim Kimya, Tekirdağ, Türkiye) was used as the flocculant in the study. The experiments were carried out in both process water and distilled water environments.

2.2. Sedimentation tests

Flocculation-assisted sedimentation tests were conducted to investigate the effects of flocculant dosage and water type on the settling behaviour of sulphide iron ore tailings. The experiments were performed using both pure water and process water with and without the addition of a flocculant. All experiments were carried out at the natural pH of the slurry (approximately 6.5). For each test, a suspension containing 30 wt.% solids was prepared and initially mixed for 5 min using a mechanical overhead stirrer to ensure complete particle dispersion. The suspension was then transferred into a 100 cm^3 graduated cylinder, after which the required volume of flocculant stock solution was added. To facilitate uniform flocculant distribution and promote floc formation while minimizing floc breakage, the

cylinder was positioned horizontally and gently tilted approximately 30° to each side for 20 cycles. This procedure provided effective mixing without applying excessive shear. After this step, the cylinder was returned to an upright position and the slurry was allowed to settle under gravity without further agitation. The interface height between the clarified supernatant and the settled solids was recorded to evaluate the sedimentation behaviour.

2.3. Turbidity measurements

To evaluate the supernatant clarity, approximately 10 cm^3 of supernatant was collected from the upper portion of the graduated cylinder at predetermined time intervals using a Pasteur pipette, and its turbidity was measured. Turbidity measurements were performed using a WTW Turb 430 turbidity meter (Xylem Analytics GMBH, Weilheim, Germany).

2.4. Zeta potential measurements

Zeta potential measurements were performed using a BeNano 180 Zeta Potential Analyzer (Bettersize Instruments, Dandong, China). Suspensions were prepared at a solid concentration of 0.1% and homogenized by magnetic stirrer for 5 min. Subsequently, 1 cm^3 of the suspension was transferred into the measurement cell, and the zeta potential was determined. The measurements were carried out over a range of pH values. The suspension pH was continuously monitored using an AB23PH-F pH meter (Ohaus Corporation, Parsippany, NJ, USA) and adjusted with analytical grade HCl or NaOH solutions as required. All measurements were conducted at room temperature (23±2^{o}C), and the standard deviation was within ±2 mV.

2.5. Floc size distribution measurements

Floc size distribution measurements were conducted to investigate the effects of flocculant dosage and water type on floc formation and temporal changes in floc stability. The experiments were performed using both pure water and process water at the slurry's natural pH. Floc size distributions were determined using a laser diffraction particle size analyzer (Malvern Mastersizer 2000, Malvern Panalytical, London, UK). Following flocculant addition and conditioning, representative suspension samples were carefully withdrawn from the sedimentation system to minimize floc breakage during sampling. The samples were then introduced into the particle size analyzer's measurement cell, and the floc size distributions were recorded.

2.6. Filtration tests

Filtration tests were performed using an in-house laboratory-scale pressure filter and the settled underflow obtained after flocculation and sedimentation. The filtration feed consisted of a 30 wt.% solids suspension. Prior to flocculation, the suspension was mixed for 5 min with a mechanical overhead stirrer to ensure complete dispersion. Flocculation was carried out at the slurry's natural pH using an anionic polyacrylamide at a dosage of 30 g/Mg. After adding the flocculant, the suspension was conditioned at 120 rpm for 2 min and then allowed to settle for 20 min. The supernatant was decanted, and the resulting settled underflow was used as the feed material for the filtration experiments. Filtration tests were conducted using a laboratory-scale pressure filter at a constant pressure of 7 bar for a total filtration time of 15 min. The effect of chamber thickness on filtration behaviour was evaluated by testing different chamber configurations. During filtration, the cumulative filtrate mass was recorded by collecting and weighing the filtrate at predetermined time intervals. After each test, the filter cake was removed and weighed wet and dry. Cake moisture content, solids content, total cake mass, dry cake mass, and cake thickness were subsequently determined.

3. Results and discussion

3.1. Effect of flocculant dosage on sedimentation behavior

Fig. 4 shows bed height changes during sedimentation tests. Without flocculant addition, the suspension settled slowly in both waters. During the first minute, the solid-liquid interface decreased

by only about 6 mm, while the bed height was reduced from the initial 215 mm to 115 mm in pure water and 114.5 mm in process water after 30 min. This behaviour is characteristic of fine-tailings suspensions, in which electrostatic repulsion between negatively charged particles stabilises the fine fraction and prevents natural aggregation (Johnson et al., 2000; Li et al., 2013; Wang et al., 2014).

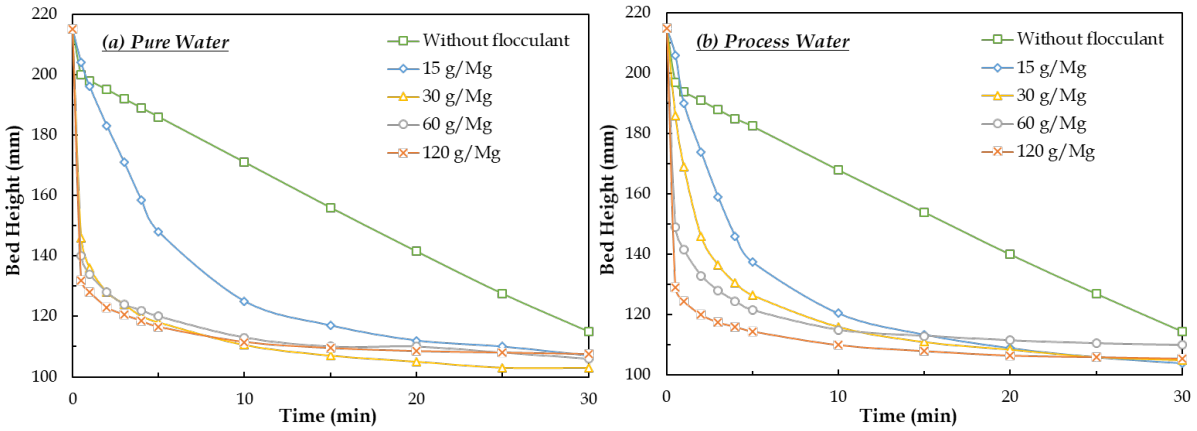

Fig. 4. Effect of flocculant dosage on sedimentation behaviour of the sample in (a) pure water and (b) process water

Flocculant addition significantly improved settling behaviour. At a dosage of 15 g/Mg, bed height boundary decreased by 19 mm in pure water and 25 mm in process water during the first minute. In pure water and process water, final bed height decreased to 107 mm and 104 mm, respectively, indicating partial aggregation. A much greater improvement was observed when the dosage increased from 15 to 30 g/Mg. At 30 g/Mg, the solid-liquid boundary moved downward by 79 mm in pure water and 46 mm in process water within the first minute. The final bed heights were 103 mm in pure water, the lowest value obtained in this study, and 105 mm in process water. This improvement can be explained by the polymer bridging mechanism, in which polymer chains adsorb onto multiple particles and form large flocs that settle rapidly once sufficient surface coverage is achieved (Gregory & Barany, 2011; Hogg, 2000). The relatively small improvement at 15 g/Mg suggests that the amount of adsorbed polymer was insufficient to form effective bridges between particles (Sworska et al., 2000a), which is consistent with previous studies on fine tailings suspensions (Arjmand et al., 2019).

Further increases in flocculant dosage to 60 and 120 g/Mg resulted in only slight improvements in the initial settling rate. During the first minute, the solid-liquid boundary moved downward by 81 and 87 mm in pure water and by 73.5 and 90.5 mm in process water, respectively. However, the final bed heights increased compared with those at 30 g/Mg, reaching 106-107.5 mm in pure water and 105.5-110 mm in process water. These results indicate that the fastest settling did not produce the most compact sediment. At high flocculant dosages, excess polymer promotes the formation of large but loosely packed flocs that retain more water. Although these flocs settle rapidly because of their larger size, they form a bulky sediment with poor consolidation characteristics (Alam et al., 2011; Hogg, 2000; Jarvis et al., 2005; Nasser & James, 2006). Therefore, based on the final bed height, 30 g/Mg provided the best balance between rapid settling and sediment compaction under the tested conditions.

3.2. Effect of flocculant dosage and water type on supernatant turbidity

Fig. 5 presents the supernatant turbidity values. Flocculant addition significantly improved clarification performance compared with the flocculant-free condition. After 30 min of settling, the turbidity was 78.8 NTU in pure water and 56.7 NTU in process water without flocculant. At a flocculant dosage of 30 g/Mg, the turbidity decreased to 35.8 NTU in pure water and 20.50 NTU in process water.

The turbidity results show that increasing the flocculant dosage from 30 to 60 g/Mg further improved the clarification performance, although no corresponding improvement was observed in sediment compaction. The lowest turbidity values after 30 min were obtained at 60 g/Mg, reaching 23.6 NTU in pure water and 6.9 NTU in process water. In process water, the turbidity had already decreased to 10.9 NTU after only 10 min, indicating rapid clarification. These results suggest that the additional

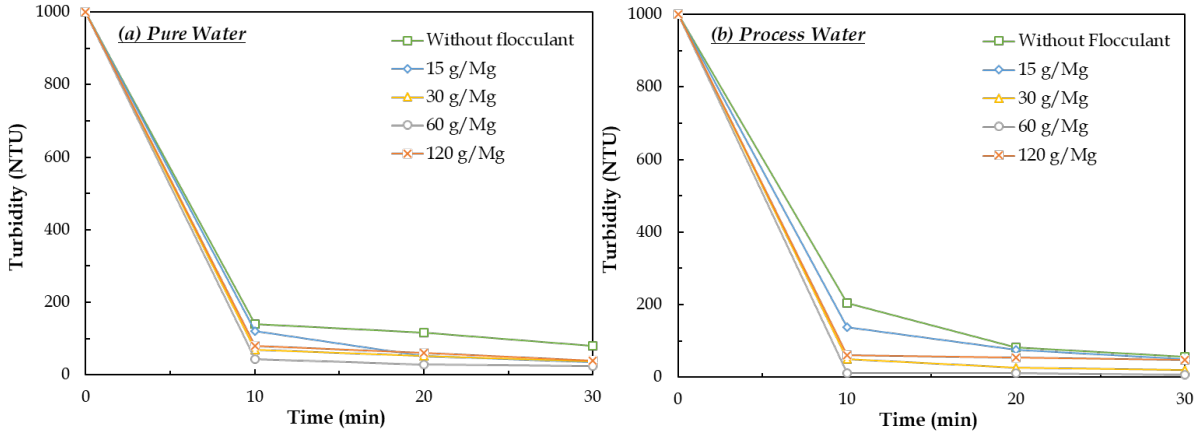

Fig. 5. Effect of flocculant dosage on supernatant turbidity of the suspension in (a) pure water and (b) process water

polymer promoted the capture of residual ultrafine particles that remained suspended at lower dosages. Although 30 g/Mg produced the most compact sediment, a slightly higher dosage was more effective for removing fine particles responsible for supernatant turbidity. Similar differences between the optimum dosages for settling, sediment consolidation, and clarification have been reported for polymer-flocculated mineral suspensions (Arjmand et al., 2019; Besra et al., 2000; Hogg, 2000).

When the flocculant dosage was further increased to 120 g/Mg, the turbidity increased to 38.5 NTU in pure water and 46.9 NTU in process water. This result indicates that excessive flocculant addition reduced the clarification efficiency. At high polymer concentrations, particle surfaces become extensively covered by adsorbed polymer, which reduces the effectiveness of polymer bridging and can lead to partial restabilization of fine particles due to steric repulsion (Alam et al., 2011; Gregory & Barany, 2011; Zhu et al., 2009). In addition, the large flocs formed at this dosage are more susceptible to breakage during mixing, releasing fine particles back into the suspension and increasing the residual turbidity. Therefore, although higher flocculant dosages may initially enhance particle capture, overdosing adversely affects clarification performance. These findings demonstrate that the optimum flocculant dosage depends on the selected performance criterion and should be determined by considering settling behaviour, sediment compaction, and supernatant clarity together.

3.3. Effect of water type on sedimentation and clarification behavior

Water type significantly affected both settling kinetics and the clarification performance, although their effects followed opposite trends. A direct comparison at the selected flocculant dosage of 30 g/Mg is presented in Fig. 6. In pure water, the bed height descended by 79 mm within the first minute. In contrast, only 46 mm of interface movement was observed in process water. Despite this slower settling behaviour, process water produced a substantially clearer supernatant after 30 min, with a turbidity of 20.5 NTU compared with 35.8 NTU in pure water. A similar trend was observed at 60 g/Mg, where the final turbidity values were 6.99 NTU in process water and 23.60 NTU in pure water. In contrast, at lower (15 g/Mg) and higher (120 g/Mg) flocculant dosages, the supernatants obtained in process water were slightly more turbid than those produced in pure water. These results demonstrate that a higher settling rate does not necessarily correspond to improved clarification efficiency. Instead, the beneficial effect of process water was evident only within the optimum flocculant dosage range, where the medium's ionic composition likely promoted more effective polymer bridging and enhanced the capture of ultrafine particles.

These observations can be explained by the two competing effects of dissolved ions on polymer-assisted flocculation. On the one hand, the elevated electrolyte concentration in the process water compresses the electrical double layer around the particles. It allows dissolved ions, particularly Ca^{2+}, to act as ionic bridges between the negatively charged mineral surfaces and the carboxylate groups of the anionic polyacrylamide. This additional coagulation mechanism destabilizes the ultrafine particles that are less efficiently captured by polymer bridging alone, and the synergistic interaction between

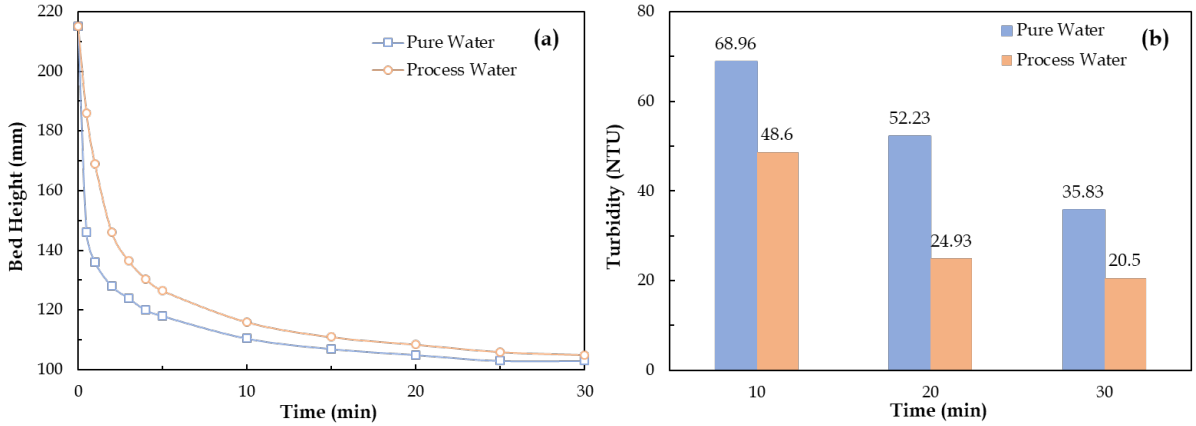

Fig. 6. Comparison of (a) bed height and (b) supernatant turbidity in pure water and process water at 30 g/Mg flocculant dosage

dissolved ions and anionic flocculants in saline media has been widely reported (Bolto & Gregory, 2007; Ozkan et al., 2016; Ramos et al., 2020; Sworska et al., 2000a). The lower turbidity of the process watersupernatant without flocculant (56.7 NTU compared with 78.8 NTU in pure water) further confirms that dissolved ions alone provide a measurable coagulating effect. In contrast, the same increase in ionic strength promotes electrostatic screening of the polymer chains, causing them to adopt a more compact shape with a shorter effective bridging length. As a result, the maximum floc size decreases and, under sufficiently high ionic strength or excessive polymer dosage, flocculation efficiency may also decline (Liu et al., 2018; Nasser & James, 2006). Similar dual effects of salinity, namely enhanced coagulation of ultrafine particles together with reduced polymer bridging efficiency, have also been reported for clay-rich tailings flocculated in saline and seawater media (Liu et al., 2018; Ramos et al., 2020).

From a practical perspective, these findings show that using recycled process water, increasingly adopted because of limited water availability and environmental regulations (Araya et al., 2021; Ossa-Moreno et al., 2018; Wang et al., 2014), does not reduce the clarification performance of the flocculation stage. Instead, within the optimum dosage range, process water produced a noticeably clearer supernatant, which is advantageous when the recovered water is recycled back to flotation. However, the dependence of the flocculation response on dosage also indicates that the balance between cation-assisted coagulation and polymer chain compaction governs clarification performance. Therefore, changes in process water chemistry resulting from seasonal variations or changes in ore composition should be monitored.

Direct evidence for the role of dissolved ions is provided by the zeta potential measurements shown in Fig. 7. In pure water, the particles remained negatively charged throughout the investigated pH range, with no isoelectric point observed between pH 2.5 and 10.7. The zeta potential decreased gradually from approximately -15 mV at pH 2.5 to approximately -32 mV at pH 10.7, reaching -26.1 mV at the natural suspension pH (≈6). This behavior is characteristic of silicate-rich mineral surfaces, where progressive deprotonation of surface hydroxyl groups increases the negative surface charge as pH rises (Johnson et al., 2000).

In contrast, the process water suspensions exhibited considerably lower zeta potential values and showed only a weak dependence on pH. Across the entire pH range, the zeta potential remained relatively constant, varying only between approximately -13 and -19 mV, with values of about -17 to -19 mV at the natural suspension pH of 6.3 to 6.5. The conductivity of the process water suspensions, ranging from 2.57 to 2.98 mS/cm, was nearly one order of magnitude higher than that of the pure water suspensions, confirming the much higher ionic strength of the recycled water. This decrease in zeta potential, along with its limited variation with pH, is consistent with compression of the electrical double layer and specific adsorption of multivalent cations onto the negatively charged particle surfaces (Liu et al., 2018; Ramos et al., 2020; Sworska et al., 2000a). The reduction in electrostatic repulsion in

process water promotes coagulation via dissolved ions and facilitates cation-polymer interactions, thereby explaining the improved clarification observed at the optimum flocculant dosage.

The conductivity of the process water suspensions approaches the range where electrophoretic mobility measurements become increasingly susceptible to experimental artifacts, including Joule heating and electrode polarization (Delgado et al., 2007). Accordingly, the values presented in Fig. 7 are reported as apparent zeta potentials. They should be interpreted primarily as indicators of the overall reduction in effective surface charge rather than as absolute values.

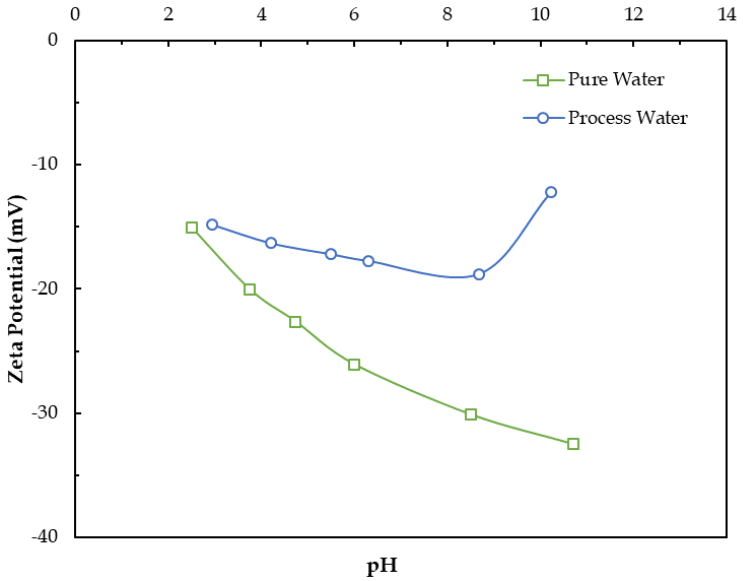

Fig. 7. Zeta potential of the sample as a function of pH in pure water and process water

3.4. Effect of flocculant dosage and water type on floc size

Table 4 presents d_{10}, d_{50}, and d_{90} values for the flocs formed at different flocculant dosages in both pure and process water. Without flocculant, d_{10}, d_{50}, and d_{90} values were 2.67, 17.49, and 63.03 µm, respectively. In pure water, d_{10} increased from 8.68 to 25.83 µm as flocculant dosage increased from 15 to 120 g/Mg. Over the same dosage range, d_{50} increased from 42.74 to 79.18 µm, while d_{90} increased from 134.75 to 176.61 µm. d_{90} value was 164.12 µm at 30 g/Mg, decreased slightly to 159.86 µm at 60 g/Mg, and then increased to 176.61 µm at 120 g/Mg. In process water, d_{10} values were 6.61, 6.64, 14.20, and 12.67 µm at flocculant dosages of 15, 30, 60, and 120 g/Mg, respectively. The corresponding d_{50} values were 37.47, 45.02, 58.41, and 51.77 µm, while the d_{90} values were 116.51, 146.10, 153.60, and 120.85 µm.

Table 4. d_{10}, d_{50}, and d_{90} values of flocs formed at different flocculant dosages in pure water and process water

Flocculant Concentration (g/Mg)	Pure Water Floc Size (µm)			Flocculant Concentration (g/Mg)	Process Water Floc Size (µm)		
	d_{10}	d_{50}	d_{90}		d_{10}	d_{50}	d_{90}
No Flocculant	2.67	17.49	63.03	*No Flocculant*	2.67	17.49	63.03
15	8.68	42.74	134.75	15	6.61	37.47	116.51
30	10.9	53.31	164.12	30	6.64	45.02	146.1
60	14.9	61.26	159.86	60	14.2	58.41	153.6
120	25.83	79.18	176.61	120	12.67	51.77	120.85

The effect of flocculant dosage on floc size distribution in pure water and process water is shown in Fig. 8. In both water, floc size distributions changed clearly with flocculant dosage. In pure water, the addition of flocculant shifted the floc size distribution toward larger particle sizes compared with the flocculant-free condition. At the lowest dosage (15 g/Mg), floc formation increased significantly, while the distribution curves obtained at 30 and 60 g/Mg were very similar, indicating only a small increase in floc size. In contrast, the distribution curve at 120 g/Mg was shifted furthest to the right, indicating

the formation of the largest flocs. In the process water medium, floc size distributions showed a different trend than in pure water. Adding a flocculant shifted all distribution curves toward larger particle sizes. However, the differences among the 15, 30, 60, and 120 g/Mg dosages became less pronounced in the coarse-particle-size region. In particular, increasing the flocculant dosage beyond 30 g/Mg produced only small increases in floc size, suggesting that most floc growth had already occurred at relatively low dosages under process water conditions. Furthermore, at every flocculant dosage, flocs formed in process water remained consistently smaller than those produced in pure water, consistent with the slower settling rates observed in the sedimentation tests. Despite their smaller size, however, the similar final sediment bed heights obtained in both waters indicate that the process water flocs were more compact and denser than those formed in pure water. The observed trends are consistent with previous studies. Increasing anionic polyacrylamide dosage promoted floc growth only up to an optimum level, beyond which polymer adsorption reached surface saturation and limited further aggregate enlargement. The present results suggest that this saturation threshold is reached at lower flocculant dosages in process water, likely because dissolved ions facilitate enhanced polymer adsorption. Furthermore, although smaller flocs were formed in process water, the final bed heights remained comparable to those obtained in pure water. This behaviour can be attributed to the formation of denser, more compact floc structures, which produce sediment beds with higher packing density despite their smaller size (Gungoren et al., 2018; Ofori et al., 2011).

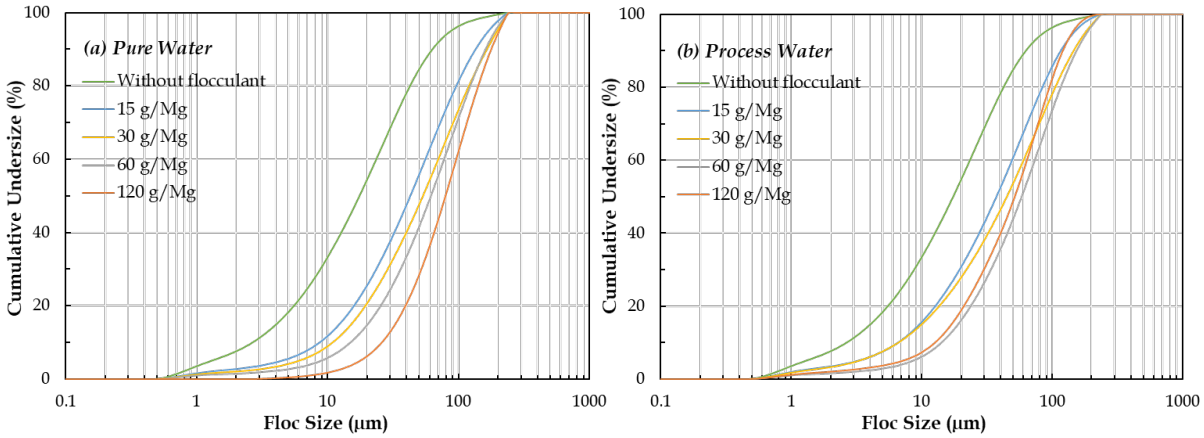

Fig. 8. Floc size distributions obtained at different flocculant dosages in (a) pure water and (b) process water

The temporal evolution of floc size (d_{90}) at different flocculant dosages is presented in Fig. 9. Prior to flocculation, the feed exhibited d_{90}, d_{50}, and d_{10} values of approximately 63, 17.5, and 2.7 µm, respectively. The addition of flocculant resulted in a rapid increase in floc size, with d_{90} increasing by approximately 2.0-2.7 times within the first minute of conditioning. In pure water, the initial floc size increased with increasing flocculant dosage. After 1 min of conditioning, d_{90} values of approximately 129, 151, 148, and 169 µm were obtained at dosages of 15, 30, 60, and 120 g/Mg, respectively, indicating that the highest dosage produced the largest initial flocs. Despite this initial trend, floc size evolved differently across the tested dosages. Between 1 and 4 min, d_{90} decreased by about 19%, 16%, and 12% at 15, 60, and 120 g/Mg, respectively. In contrast, only a 3% reduction was observed at 30 g/Mg, with d_{90} decreasing from 151 to 146 µm. Although the 30 g/Mg dosage did not yield the largest initial flocs, it produced the most structurally stable flocs, exhibiting the greatest resistance to hydrodynamic stresses encountered during handling and particle-size measurements.

In process water, the floc sizes obtained at dosages of 30, 60, and 120 g/Mg became similar, reaching a relatively narrow range of approximately 145 to 147 µm after 1 min of stirring. After 4 min of measurement, the largest flocs were observed at 30 g/Mg, with a d_{90} of approximately 136 µm, whereas the corresponding values at 60 and 120 g/Mg were only 129-131 µm. These results highlight two important features of the flocculation behaviour in process water. First, the limited increase in floc size at dosages above 30 g/Mg indicates that, under saline conditions, floc growth was controlled primarily by limited polymer-chain extension rather than polymer availability. This agrees with previous studies showing that increasing ionic strength causes polymer chains to adopt a more compact configuration

because dissolved ions reduce electrostatic repulsion, shorten the effective bridging distance, and limit further aggregate growth. Second, the highest flocculant dosage (120 g/Mg) exhibited a clear delay in floc growth. In pure water, the maximum floc size was reached immediately after stirring and then gradually decreased during the measurement period. The delayed floc growth observed in process water is consistent with the slower extension, adsorption, and rearrangement of polymer chains, which are affected by electrostatic screening on mineral surfaces in saline media (Nasser & James, 2006).

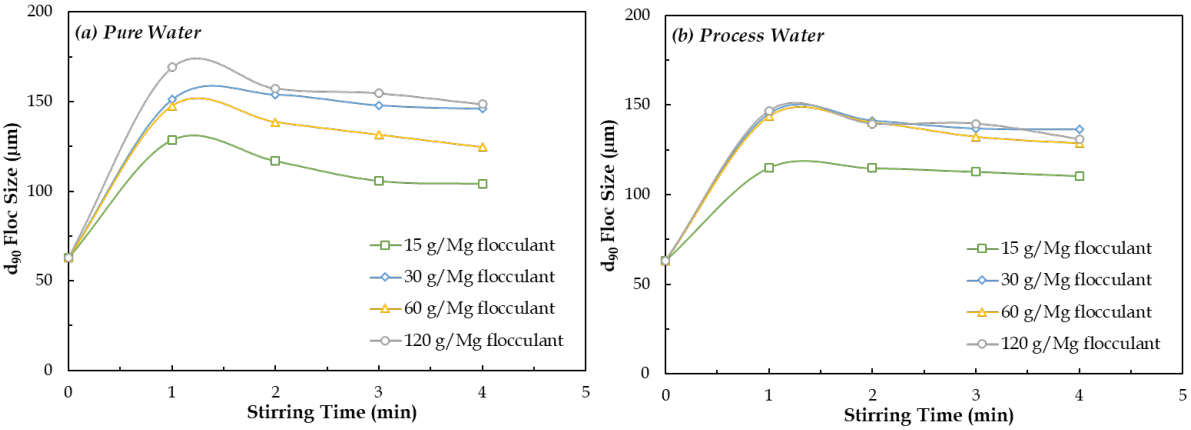

Fig. 9. Evolution of d_{90} floc size as a function of time at different flocculant dosages in (a) pure water and (b) process water

A gradual reduction in floc size at higher flocculant dosages indicates shear-induced breakage of relatively large and loosely bound flocs. Previous studies have shown that floc strength generally decreases as floc size increases, making oversized flocs formed under overdosing conditions more susceptible to fragmentation while exhibiting only limited reflocculation after breakage (Hogg, 2000; Jarvis et al., 2005; Sworska et al., 2000b). Similarly, studies monitoring changes over time have shown that tailings flocculated in seawater continue to evolve for several minutes after polymer addition, as shear-induced breakage occurs simultaneously with the development of a more compact floc structure (Leiva et al., 2021). The behaviour observed in this study aligns closely with these findings. Although the 60 and 120 g/Mg dosages initially produced flocs comparable to or larger than those formed at 30 g/Mg, the moderately sized flocs formed at 30 g/Mg remained more stable. As a result, they settled more rapidly, formed the most compact sediment bed, and retained ultrafine particles more effectively. The larger flocs produced at 60 g/Mg, and particularly at 120 g/Mg, were more vulnerable to shear-induced breakage. Their fragmentation generated a more porous sediment structure and released previously captured ultrafine particles into the supernatant, leading to the subsequent increase in turbidity.

3.5. Effect of chamber thickness on filtration behaviour of the flocculated tailings

Fig. 10 shows the cumulative filtrate recovery and final cake moisture obtained at different chamber thicknesses. Chamber thickness clearly affected cumulative filtrate recovery: the 40 mm chamber consistently produced the highest recovery throughout the filtration period, while the 25- and 32-mm chambers performed nearly identically. In contrast, chamber thickness had a relatively small influence on final cake moisture. Final cake moisture ranged from 28.18% to 29.58%, with the 32 mm chamber producing the lowest moisture and only minor differences among the three chamber thicknesses. These results indicate that increasing chamber thickness primarily enhances the amount of water recovered during each filtration cycle, whereas its effect on the residual cake moisture is limited. Therefore, chamber thickness influences water recovery more strongly than the final cake moisture under the constant-pressure filtration conditions investigated.

Greater cumulative filtrate recovery should not be considered direct evidence of better dewatering performance. Previous studies have demonstrated that thinner cakes generally produce lower residual moisture contents and higher specific filter capacities despite yielding lower absolute filtrate volumes

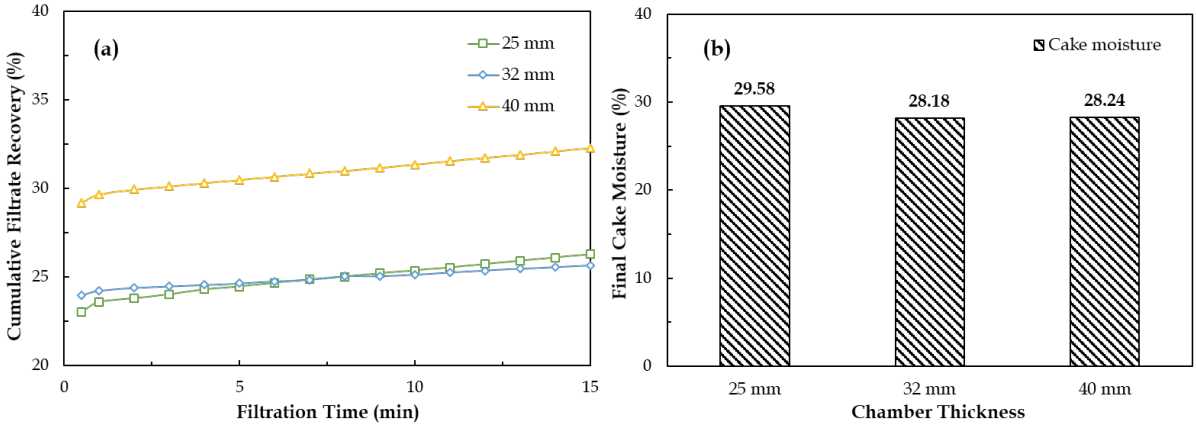

Fig. 10. Effect of chamber thickness on (a) cumulative filtrate recovery during pressure filtration and on (b) the final cake moisture of a slurry flocculated with 30 g/Mg flocculant

per cycle. For example, Raman & Klima (2018) reported that reducing cake thickness during filtration under constant pressure of fine coal refuse simultaneously decreased final cake moisture and increased specific filtration capacity. Similar trends have been reported for various mineral tailings and coal slurries, where shorter drainage paths and lower overall cake resistance in thinner cakes result in shorter cycle times, whereas thicker cakes maximise water recovery per cycle but delay reaching the desired cake moisture (Alam et al., 2011; Luo et al., 2024; Wakeman, 2007). Accordingly, the nearly identical recoveries from the 25- and 32-mm chambers, together with the considerably higher recovery from the 40-mm chamber, illustrate the well-known balance in filter-press operation. Increasing chamber depth enhances per-cycle water recovery, whereas thinner chambers generally provide greater long-term processing capacity and lower residual cake moisture.

From an operational perspective, the optimal chamber thickness for tailings should be selected based on the primary objective of the dewatering circuit. If maximising water recovery per filtration cycle is the main objective, such as in operations where process water recycling is critical under water-limited conditions, the 40 mm chamber offers a clear advantage. In contrast, when minimising cake moisture, shortening cycle time, and maximising filter capacity are of greater importance, as is typically the case in dry-stack tailings management, the 25 and 32 mm chamber configurations are expected to provide a more favourable balance between dewatering efficiency and overall process productivity (Fränkle et al., 2024; Raman & Klima, 2018).

4. Conclusions

This study evaluated the combined effects of flocculant dosage and water chemistry on the sedimentation, floc evolution, and pressure filtration behaviour of sulphide iron ore tailings. Flocculant addition significantly improved both settling and clarification compared with the unconditioned suspension. The greatest improvement was achieved by increasing the dosage from 15 to 30 g/Mg, whereas further increases provided limited additional benefit or reduced dewatering performance.

Among the dosages investigated, 30 g/Mg produced the most compact sediment bed and the most shear-resistant flocs, maintaining an almost constant d_{90} during the 1 to 4 min stirring period. Although increasing the dosage to 60 g/Mg further improved supernatant clarity, particularly in process water, it slightly reduced sediment consolidation. At 120 g/Mg, excessive polymer addition partially restabilized the suspension and increased floc breakage, resulting in significantly higher supernatant turbidity.

Water chemistry influenced settling and clarification in different ways. Pure water promoted faster interface settling in all tests, whereas process water produced lower turbidity only at intermediate flocculant dosages (30 to 60 g/Mg). Obtained zeta potential measurements confirmed that the higher ionic strength of the process water reduced the magnitude of the particle surface charge, indicating electrical double-layer compression. The improved clarification observed under these conditions is

attributed to enhanced aggregation by dissolved cations. At the same time, the reduced floc growth at higher dosages reflects polymer chain contraction under elevated ionic strength.

Floc size measurements further demonstrated that floc stability, rather than initial floc size, governed overall dewatering performance. Although the highest dosage produced the largest initial flocs, only the 30 g/Mg condition produced flocs that remained resistant to shear during conditioning, highlighting the importance of floc durability for effective sedimentation.

Pressure filtration results showed that increasing chamber thickness increased cumulative filtrate recovery, reaching 32.30% for the 40 mm chamber, while the final cake moisture remained nearly unchanged across all chamber configurations. This indicates that thicker chambers maximise water recovery per filtration cycle, whereas thinner chambers remain advantageous when shorter cycle times and higher specific filter capacity are prioritised.

Overall, a flocculant dosage of 30 g/Mg provided the most balanced performance, combining rapid settling, effective sediment consolidation, high floc stability, and favourable filtration behaviour. The results also demonstrate that recycled process water can be used without compromising dewatering performance and can improve clarification under appropriate flocculation conditions. These findings provide practical guidance for optimising flocculation and filtration operations in mineral processing plants while supporting more sustainable water management practices.

Acknowledgments

This research was funded by the Office of Scientific Research Projects of Istanbul Technical University, grant number MYL-2025-47336.

A part of the results reported in this paper were presented at XX Balkan Mineral Processing Congress BMPC 2026 entitled "Effect of flocculant dosage and water type on the sedimentation behavior of sulfide iron ore tailings".

References

ALAM, N., OZDEMIR, O., HAMPTON, M.A., NGUYEN, A.V., 2011. *Dewatering of coal plant tailings: Flocculation followed by filtration.* Fuel, 90(1), 26-35. https://doi.org/10.1016/j.fuel.2010.08.006

AMARANTE, S.C., ARAUJO, A.C., VALADÃO, G.E.S., PERES, A.E.C., 2002. *Cake dewatering of some iron ore industrial products.* Mining, Metallurgy & Exploration, 19(3), 161-164. https://doi.org/10.1007/BF03403169

ARAYA, N., RAMÍREZ, Y., KRASLAWSKI, A., CISTERNAS, L.A., 2021. F*easibility of re-processing mine tailings to obtain critical raw materials using real options analysis.* Journal of Environmental Management, 284, 112060. https://doi.org/10.1016/j.jenvman.2021.112060

ARJMAND, R., MASSINAEI, M., BEHNAMFARD, A., 2019. *Improving flocculation and dewatering performance of iron tailings thickeners.* Journal of Water Process Engineering, 31, 100873. https://doi.org/10.1016/j.jwpe.2019.100873

BESRA, L., SENGUPTA, D.K., ROY, S.K., 2000. *Particle characteristics and their influence on dewatering of kaolin, calcite and quartz suspensions.* International Journal of Mineral Processing, 59(2), 89-112. https://doi.org/10.1016/S0301-7516(99)00065-4

BOLTO, B., GREGORY, J., 2007. *Organic polyelectrolytes in water treatment.* Water Research, 41(11), 2301-2324. https://doi.org/10.1016/j.watres.2007.03.012

DASH, M., DWARI, R.K., BISWAL, S.K., REDDY, P.S.R., CHATTOPADHYAY, P., MISHRA, B.K., 2011. *Studies on the effect of flocculant adsorption on the dewatering of iron ore tailings.* Chemical Engineering Journal, 173(2), 318-325. https://doi.org/10.1016/j.cej.2011.07.034

DELGADO, Á.V., GONZÁLEZ-CABALLERO, F., HUNTER, R.J., KOOPAL, L.K., LYKLEMA, J., 2007. *Measurement and interpretation of electrokinetic phenomena.* Journal of colloid and interface science, 309(2), 194-224.

DIAS, C.L.P., VALADÃO, G.E.S., ARAUJO, A.C., PERES, A.E.C., AMARANTE, S.C., 2003. *The effect of reagents on ultrafine iron ore vacuum filtration.* Filtration & Separation, 40(5), 36-39. https://doi.org/10.1016/S0015-1882(03)00532-9

FRÄNKLE, B., SOK, T., GLEIß, M., NIRSCHL, H., 2024. *Copper tailings filtration: Influence of filter cake desaturation*. Minerals Engineering, 217, 108952. https://doi.org/10.1016/j.mineng.2024.108952

GREGORY, J., BARANY, S., 2011. *Adsorption and flocculation by polymers and polymer mixtures.* Advances in Colloid and Interface Science, 169(1), 1-12. https://doi.org/10.1016/j.cis.2011.06.004

GUNGOREN, C., BAKTARHAN, Y., KURSUN, I., OZKAN, S.G., OZDEMIR, O., 2018. *Characterization of flocs in dewatering of coal plant tailings*. Hittite Journal of Science and Engineering, 5(3), 215-218. https://doi.org/10.17350/HJSE19030000097

GUNGOREN, C., KURSUN, I., OZDEMIR, O., 2020. *Investigation of flocculation properties and floc structure of coal processing plant tailings in the presence of monovalent and divalent ions.* Physicochemical Problems of Mineral Processing, 56(5), 747-758. https://doi.org/10.37190/ppmp/125070

HÄKKINEN, A., EKBERG, B., 2009. *Dewatering of iron ore slurry by a ceramic vacuum disc filter.* Chemical Engineering Transactions, 17, 1431-1436. https://doi.org/10.3303/CET0917239

HOGG, R., 2000. *Flocculation and dewatering*. International Journal of Mineral Processing, 58(1-4), 223-236. https://doi.org/10.1016/S0301-7516(99)00023-X

JARVIS, P., JEFFERSON, B., GREGORY, J., PARSONS, S.A., 2005. *A review of floc strength and breakage.* Water Research, 39(14), 3121-3137. https://doi.org/10.1016/j.watres.2005.05.022

JOHNSON, S.B., FRANKS, G.V., SCALES, P.J., BOGER, D.V., HEALY, T.W., 2000. *Surface chemistry-rheology relationships in concentrated mineral suspensions.* International Journal of Mineral Processing, 58(1-4), 267-304. https://doi.org/10.1016/S0301-7516(99)00041-1

LEE, D.J., LAI, J.Y., MUJUMDAR, A.S., 2006. *Moisture distribution and dewatering efficiency for wet materials.* Drying Technology, 24(10), 1201-1208. https://doi.org/10.1080/07373930600838041

LEIVA, W.H., FAWELL, P.D., GOÑI, C., TORO, N., JELDRES, R.I., 2021. *Temporal evolution of the structure of tailings aggregates flocculated in seawater.* Minerals Engineering, 160, 106708. https://doi.org/10.1016/j.mineng.2020.106708

LI, J., JIAO, S., ZHONG, L., PAN, J., MA, Q., 2013. *Optimizing coagulation and flocculation process for kaolinite suspension with chitosan.* Colloids and Surfaces A: Physicochemical and Engineering Aspects, 428, 100-110. https://doi.org/10.1016/j.colsurfa.2013.03.034

LIU, D., EDRAKI, M., BERRY, L., 2018. *Investigating the settling behaviour of saline tailing suspensions using kaolinite, bentonite, and illite clay minerals.* Powder Technology, 326, 228-236. https://doi.org/10.1016/j.powtec.2017.11.070

LUO, Y., EKANAYAKE, N.I.K., AMINI, N., MOON, E., HAPGOOD, K., SCALES, P.J., & STICKLAND, A.D., 2024. *Quantifying the effects of clays on mineral tailings filtration.* Minerals Engineering, 216, 108830. https://doi.org/10.1016/j.mineng.2024.108830

MCGUIRE, M.J., ADDAI-MENSAH, J., BREMMELL, K.E., 2006. *The effect of polymer structure type, pH and shear on the interfacial chemistry, rheology and dewaterability of model iron oxide dispersions.* Colloids and Surfaces A: Physicochemical and Engineering Aspects, 275(1-3), 153-160. https://doi.org/10.1016/j.colsurfa.2005.09.034

NASSER, M.S., JAMES, A.E., 2006. *The effect of polyacrylamide charge density and molecular weight on the flocculation and sedimentation behaviour of kaolinite suspensions.* Separation and Purification Technology, 52(2), 241-252. https://doi.org/10.1016/j.seppur.2006.04.005

NEGRO, C., SÁNCHEZ, L.M., FUENTE, E., BLANCO, Á., TIJERO, J., 2006. *Polyacrylamide induced flocculation of a cement suspension*. Chemical Engineering Science, 61(8), 2522-2532. https://doi.org/10.1016/j.ces.2005.11.013

OFORI, P., NGUYEN, A.V., FIRTH, B., MCNALLY, C., OZDEMIR, O., 2011. *Shear-induced floc structure changes for enhanced dewatering of coal preparation plant tailings*. Chemical Engineering Journal, 172(2-3), 914-923. https://doi.org/10.1016/j.cej.2011.06.082

OSSA-MORENO, J., MCINTYRE, N., ALI, S., SMART, J.C.R., RIVERA, D., LALL, U., KEIR, G., 2018. *The hydro-economics of mining.* Ecological Economics, 145, 368-379. https://doi.org/10.1016/j.ecolecon.2017.11.010

OZKAN, A., ONER, B., ONEN, V., DUZYOL, S., 2016. *Flocculation of coal suspension with mono/dual polymer systems and contribution of Ca(II)/Mg(II) ions.* Separation Science and Technology, 51(1), 106-114. https://doi.org/10.1080/01496395.2015.1085876

PALOMINO, D., HUNKELER, D., STOLL, S., 2012. *Salt concentration influence on the efficiency of two cationic polymeric flocculants.* Colloid and Polymer Science, 290(13), 1301-1308. https://doi.org/10.1007/s00396-012-2653-7

PAREKH, B.K., 2009. *Dewatering of fine coal and refuse slurries-problems and possibilities.* Procedia Earth and Planetary Science, 1(1), 621-626. https://doi.org/10.1016/j.proeps.2009.09.098

QI, Y., THAPA, K.B., HOADLEY, A.F.A., 2011. *Application of filtration aids for improving sludge dewatering properties - A review.* Chemical Engineering Journal, 171(2), 373-384. https://doi.org/10.1016/j.cej.2011.04.060

RAMAN, G.S.S., KLIMA, M.S., 2018. *Effects of cake thickness and pressure on the filtration of coal refuse slurry*. Minerals & Metallurgical Processing, 35(3), 125-132. https://doi.org/10.19150/mmp.8461

RAMOS, J.J., LEIVA, W.H., CASTILLO, C.N., IHLE, C.F., FAWELL, P.D., JELDRES, R.I., 2020. *Seawater flocculation of clay-based mining tailings: Impact of calcium and magnesium precipitation.* Minerals Engineering, 154, 106417. https://doi.org/10.1016/j.mineng.2020.106417

SWORSKA, A., LASKOWSKI, J.S., CYMERMAN, G., 2000a. *Flocculation of the Syncrude fine tailings Part I. Effect of pH, polymer dosage and Mg2q and Ca2q cations.* International Journal of Mineral Processing, 60(2), 143-152. https://doi.org/10.1016/S0301-7516(00)00012-0

SWORSKA, A., LASKOWSKI, J.S., CYMERMAN, G., 2000b. *Flocculation of the Syncrude fine tailings Part II. Effect of hydrodynamic conditions.* International Journal of Mineral Processing, 60(2), 153-161. https://doi.org/10.1016/S0301-7516(00)00013-2

WAKEMAN, R., 2007. *The influence of particle properties on filtration.* Separation and Purification Technology, 58(2), 234-241. https://doi.org/10.1016/j.seppur.2007.03.018

WANG, C., HARBOTTLE, D., LIU, Q., XU, Z., 2014. *Current state of fine mineral tailings treatment: A critical review on theory and practice.* Minerals Engineering, 58, 113-131. https://doi.org/10.1016/j.mineng.2014.01.018

ZHU, Z., LI, T., LU, J., WANG, D., YAO, C., 2009. *Characterization of kaolin flocs formed by polyacrylamide as flocculation aids.* International Journal of Mineral Processing, 91(3-4), 94-99. https://doi.org/10.1016/j.minpro.2009.01.003